WELL-BALANCED SCHEME FOR SHALLOW WATER EQUATIONS WITH ARBITRARY TOPOGRAPHY

MAI DUC THANH, MD. FAZLUL KARIM, AND AHMAD IZANI MD. ISMAIL

ABSTRACT. We study the one-dimensional shallow water equations with arbitrary topography. We first verify that traditional discretizations of the right-hand side of the equation of the balance of momentum give unsatisfactory results. We then show that the equations can be written in the divergence form for stationary waves. Motivated by the encouraging results for the well-balanced scheme for fluid flows in a nozzle with variable cross-section in [15], we construct a numerical scheme based on stationary waves. This scheme is constructed so that it maintains equilibrium states. Tests show that our scheme is both stable and fast.

CONTENTS

2000 *Mathematics Subject Classification.* 35L65, 76N10, 76L05.
Key words and phrases. Shallow water, conservation law, well-balanced scheme, topography.
Preprint, Department of Mathematics, International University, Ho Chi Minh City.

1. Introduction

We consider in this paper the numerical treatments for the following one-dimensional shallow water equations

$$\begin{aligned}
&\partial_t h + \partial_x (hu) = 0,\\
&\partial_t (hu) + \partial_x (h(u^2 + g\frac{h}{2})) = -gh\partial_x a,
\end{aligned} \tag{1.1}$$

where h is the height of the water from the bottom to the surface, u is the velocity, g is the gravity constant, and a is the height of the river bottom from a given level.

Since the topography may admit discontinuity, the system (1.1) is of *nonconservative form.* Introducing the trivial equation

$$\partial_t a = 0$$

produces another linearly degenerate characteristic field transforming the nonconservative system to a non-strictly hyperbolic system. As shown in [20], the system then lacks uniqueness as well as existence. Exact Riemann solutions of the system were constructed in [20]. Related studies of the system can be found in [21, 12, 13, 8, 19, 1, 19].

It has been shown that for nonconservative systems, or systems with source terms, traditional discretizations of the right-hand side do not give satisfactory results. In particular, oscillations may appear or the errors may grow when the mesh size is reduced. This was observed in the scalar case, see [5], and in the case of systems for the modeling of flows in a nozzle with variable cross-section, see [15]. In the case of scalar conservation laws, well-balanced schemes have been constructed, see [10, 11, 4, 9, 5, 6, 3, 14].

In this paper we will develop the idea of using stationary wave in the case of system of balance laws [15] for the shallow water equations. We then provide the tests which show the efficiency of our scheme.

2. Basic properties and stationary waves

In this section we recall basic properties of system (1.1) and stationary waves, as well as the curve of stationary waves. This is the basic component of the scheme constructed in the next section.

2.1. Basic properties of the system.

Basic properties of the system. Supplementing the system (1.1) with the trivial equation

$$\partial_t a = 0$$

the system (1.1) becomes

$$\begin{aligned}
&\partial_t h + u\partial_x h + h\partial_x u = 0,\\
&\partial_t u + g\partial_x h + u\partial_x u + g\partial_x a = 0,\\
&\partial_t a = 0
\end{aligned} \tag{2.1}$$

Setting the variable $U = (h, u, a)$, we can re-write the system (2.1) in the the nonconservative form

$$\partial_t U + A(U)\partial_x U = 0, \tag{2.2}$$

where the Jacobian matrix $A(U)$ is given by

$$A(U) = \begin{pmatrix} u & u & 0 \\ g & u & g \\ 0 & 0 & 0 \end{pmatrix}.$$

The eigenvalues of $A(U)$ satisfy

$$|A(U) - \lambda I| = 0$$

which gives

$$\lambda_1(U) := u - \sqrt{gh} < \lambda_2(U) := u + \sqrt{gh}, \quad \lambda_3(U) := 0, \tag{2.3}$$

together with the corresponding eigenvectors

$$\begin{aligned} &r_1(U) := (h, -\sqrt{gh}, 0)^t, \quad r_2(U) := (h, \sqrt{gh}, 0)^t, \\ &r_3(U) := (gh, -gu, u^2 - gh)^t. \end{aligned} \tag{2.4}$$

The first and the third characteristic fields may coincide. Indeed, letting

$$(\lambda_1(U), r_1(U)) = (l_3(U), r_3(U))$$

we obtain a hyper-surface of the space (h, u, a) on which the first and the third characteristic fields coincide

$$\mathcal{C}_+ := \{(h, u, a) | \quad u = \sqrt{gh}\}. \tag{2.5}$$

Similarly, the second and the third characteristic fields may coincide:

$$(\lambda_2(U), r_2(U)) = (l_3(U), r_3(U))$$

on the hyper-surface of the space (h, u, a)

$$\mathcal{C}_- := \{(h, u, a) | \quad u = -\sqrt{gh}\}. \tag{2.6}$$

Therefore, the system lacks strict hyperbolicity.

On the other hand, the third characteristic field (λ_3, r_3) is linearly degenerate. We have

$$-\nabla\lambda_1(U) \cdot r_1(U) = \nabla\lambda_2(U) \cdot r_2(U) = \frac{3}{2}\sqrt{gh} \neq 0, \quad h > 0.$$

The last conclusion implies that the first and the second characteristic fields (λ_1, r_1), (λ_2, r_2) are genuinely nonlinear in the open half-space $\{(h, u, a) | \quad h > 0\}$.

Now, it is convenient to set

$$\mathcal{C} = \mathcal{C}_+ \cup \mathcal{C}_- = \{(h, u, a) | \quad u^2 - gh = 0\},$$

which is the hyper-surface on which the system fails to be strictly hyperbolic.

We have seen that the system lacks strict hyperbolicity only on the surface $\mathcal{C}$. However, this surface divides the phase domain into three sub-domains

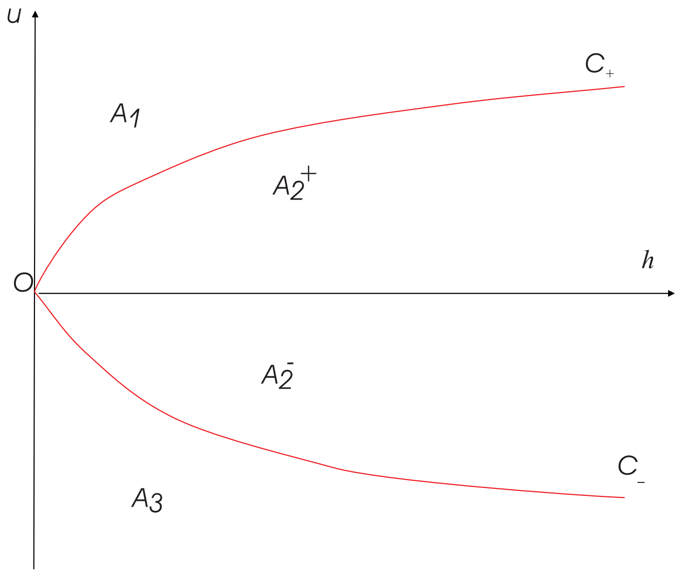

FIGURE 1. Projection of strictly hyperbolic areas in the (h, u)-plane

which are disjoint regions, or areas, denoted by A_1, A_2 and A_3, so that in each region the system is strictly hyperbolic. More precisely,

$$\begin{aligned} A_1 &:= \{(h,u,a) \in \boldsymbol{R}_+ \times \boldsymbol{R} \times \boldsymbol{R}_+ | \quad \lambda_2(U) > \lambda_1(U) > \lambda_3(U)\}, \\ A_2 &:= \{(h,u,a) \in \boldsymbol{R}_+ \times \boldsymbol{R} \times \boldsymbol{R}_+ | \quad \lambda_2(U) > \lambda_3(U) > \lambda_1(U)\}, \\ A_2^+ &:= \{(h,u,a) \in A_2 | \quad u > 0\}, \\ A_2^- &:= \{(h,u,a) \in A_2 | \quad u < 0\}, \\ A_3 &:= \{(h,u,a) \in \boldsymbol{R}_+ \times \boldsymbol{R} \times \boldsymbol{R}_+ | \quad \lambda_3(U) > \lambda_2(U) > \lambda_1(U)\}. \end{aligned} \tag{2.7}$$

2.2. **The curve of stationary waves.** Stationary waves are time-independent solutions. So stationary waves of (1.1) satisfy

$$\begin{aligned} &(hu)' = 0, \\ &\Big(\frac{u^2}{2} + g(h+a)\Big)' = 0, \end{aligned} \tag{2.8}$$

where "′" stands for the derivative with respect to x. Trajectories of the system of two differential equations (2.8) passing through each point (h_0, u_0, a_0) can be obtained easily and satisfy

$$\begin{aligned} &hu = h_0 u_0, \\ &\frac{u^2}{2} + g(h+a) = \frac{u_0^2}{2} + g(h_0 + a_0). \end{aligned} \tag{2.9}$$

The trajectories of (2.8) can be expressed in the form $u = u(h), a = a(h)$. Now, letting $h \to h_\pm$ and setting $u_\pm = u(h_\pm), a_\pm = a(h_\pm)$, we see that the states $(h_\pm, u_\pm, a_\pm)$ satisfy the jump conditions

$$\begin{aligned}&[hu] = 0,\\ &[\frac{u^2}{2} + g(h+a)] = 0,\end{aligned} \tag{2.10}$$

From (2.10), we can define a curve parameterized in h:

$$\begin{aligned}\mathcal{W}_0(U_0):\quad & u = u(h) = \frac{h_0 u_0}{h},\\ & a = a(h) = a_0 + \frac{u^2 - u_0^2}{2g} + h - h_0.\end{aligned} \tag{2.11}$$

Substitute for u in the second equation of (2.11), and re-arranging terms, we obtain

$$\begin{aligned}& u = \frac{h_0 u_0}{h},\\ & a_0 - a + \frac{u_0^2}{2g}\Big(\frac{h_0^2}{h^2} - 1\Big) + h - h_0 = 0.\end{aligned}$$

Thus, to determine the the other state of a stationary wave, given one state, we look for zeros of the function

$$\varphi(h) = a_0 - a + \frac{u_0^2}{2g}\Big(\frac{h_0^2}{h^2} - 1\Big) + h - h_0. \tag{2.12}$$

Set

$$\begin{aligned}& h_{\min}(U_0) := \Big(\frac{u_0^2 h_0^2}{g}\Big)^{1/3},\\ & a_{\min}(U_0) := a_0 + \frac{u_0^2}{2g}\Big(\frac{h_0^2}{h_{\min}^2} - 1\Big) + h_{\min} - h_0.\end{aligned}$$

Properties of the function φ in (2.12) are observed in [20].

Lemma 2.1. (Lemma 3.1, [20]) *Suppose $u_0 \neq 0$. The function $\varphi(h), h > 0$ is smooth, convex, is decreasing in the interval $(-\infty, h_{\min})$ and is increasing in the interval $(h_{\min}, \infty)$, and satisfies the limit conditions*

$$\lim_{h\to 0} \varphi(h) = \lim_{h\to\infty} \varphi(h) = \infty.$$

Consequently, if $a \geq a_{\min}$, the function φ has two zeros $h_*(U_0, a), h^*(U_0, a)$ such that $h_*(U_0, a) \leq h_{\min}(U_0) \leq h^*(U_0, a)$. The inequalities are strict whenever $a > a_{\min}(U_0)$.

As shown in [20] the Riemann problem for (1.1) may admit up to a one-parameter family of solutions. This phenomenon can be avoided by requiring Riemann solutions to satisfy a monotone condition on the component a.

(MC) (Monotonicity Criterion) - Along any stationary curve $\mathcal{W}_3(U_0)$, the bottom level a is monotone as a function of h.

A similar criterion was used by Isaacson and Temple [12, 13], LeFloch and Thanh [19, 20], and by Goatin and LeFloch [8].

It is not difficult to check that under the Monotonicity Criterion, a stationary wave from a given state $U_0 \in A_1 \cup A_3$ picks up the value $h_*(U_0, a)$ given by Lemma 2.1 to arrive at a state (h, u, a), where $h = h_*(U_0, a)$ u is given by (2.11), while a stationary wave from a given state $U_0 \in A_2$ picks up the value $h^*(U_0, a)$ given by Lemma 2.1 to arrive at a state (h, u, a), where $h = h^*(U_0, a)$ u is given by (2.11). See [20] for the proof.

3. Numerical schemes

In this section we will present a new scheme for approximating solutions of the system (1.1), relying on the arguments in the previous sections. Given a uniform time step Δt and a special mesh size Δx, setting $x_j = j\Delta x, j \in \mathbf{Z}$, and $t_n = n\Delta t, n \in \mathbf{N}$, we denote by U_j^n in what follows as the approximation of the values $U(x_j, t_n)$ of the exact solution $U = (h, hu)$ of (1.1).

Set

$$\lambda = \frac{\Delta t}{\Delta x}.$$

Let us take any standard finite difference scheme for gas dynamics equations with the numerical flux g^{C}. The *classical scheme* is of the form

$$U_j^{n+1} = U_j^n - \lambda\Big(g^{\mathrm{C}}\big(U_j^n, U_{j+1}^n\big) - g^{\mathrm{C}}\big(U_{j-1}^n, U_j^n\big)\Big) + \frac{\lambda}{2}\big(0, -gh_j^n(a_{j+1} - a_{j-1})\big)^T, \tag{3.1}$$

where $a_j := a(x_j)$. The *modified Lax–Friedrichs scheme* is of the form (3.1) with the Lax–Friedrichs numerical flux:

$$\begin{aligned} &g^{\mathrm{C}}(U, V) := \frac{1}{2}(f(U) + f(V)) - \frac{1}{2\lambda}(V - U), \\ &U := (h, hu), \quad f(U) := (hy, h(u^2 + gh/2)). \end{aligned} \tag{3.2}$$

The constant λ is also required to satisfy the so-called *CFL stability condition*

$$\lambda \max_U |f'(U)| \le 1. \tag{3.3}$$

The well-balanced scheme is defined by

$$U_j^{n+1} = U_j^n - \lambda\big(g^{\mathrm{N}}(U_j^n, U_{j+1,-}^n) - g^{\mathrm{N}}(U_{j-1,+}^n, U_j^n)\big), \tag{3.4}$$

where $g^{\mathrm{N}}(U, V)$ can be any standard numerical flux for gas dynamics equations, and $U_{j+1,-}^n, U_{j-1,+}^n$ are given below. In the next section devoted to numerical tests, we take the Lax–Friedrichs numerical flux:

$$\begin{aligned} &g^{\mathrm{N}}(U, V) := g^{\mathrm{C}}(U, V) = \frac{1}{2}\big(f(U) + f(V)\big) - \frac{1}{2\lambda}(V - U), \\ &U := (h, hu), \quad f(U) := (hy, h(u^2 + gh/2)). \end{aligned}$$

In the scheme (3.4), the states

$$U_{j+1,-}^n = (h, hu)_{j+1,-}^n, \quad U_{j-1,+}^n = (h, hu)_{j-1,+}^n$$

are defined by observing that the entropy is constant across each stationary jump, and by computing $h^n_{j+1,-}, u^n_{j+1,-}$ from the equations

$$\begin{aligned} &h^n_{j+1}u^n_{j+1} = h^n_{j+1,-}u^n_{j+1,-}, \\ &\frac{(u^n_{j+1})^2}{2} + g(h^n_{j+1} + a^n_{j+1}) = \frac{(u^n_{j+1,-})^2}{2} + g(h^n_{j+1,-} + a^n_{j+1,-}), \end{aligned} \tag{3.5}$$

and computing $h^n_{j-1,+}, u^n_{j-1,+}$ from the equations

$$\begin{aligned} &h^n_{j-1}u^n_{j-1} = h^n_{j-1,+}u^n_{j-1,+}, \\ &\frac{(u^n_{j-1})^2}{2} + g(h^n_{j-1} + a^n_{j-1}) = \frac{(u^n_{j-1,+})^2}{2} + g(h^n_{j-1,+} + a^n_{j-1,+}), \end{aligned} \tag{3.6}$$

4. Test cases

In this section we will provide some test cases to demonstrate the efficiency of our new scheme (3.4) by using MATLAB. We compute solutions by using the modified Lax–Friedrichs scheme (3.1)–(3.2) and the new scheme (3.4). Then, we compare the numerical solutions with the corresponding exact solutions, which were obtained in [20].

For all test cases, the exact solutions are available (see also [20]) and we will compute the error and the corresponding CPU times. Let us denote the unknown function to be $U = (h, u)$. The notation $U_h^{\mathrm{C}}, U_h^{\mathrm{N}}$ refer to Lax–Friedrichs solutions obtained by (3.1)–(3.2) and the new scheme (3.4), respectively.

Solutions $U(x,t)$ of the Riemann problem for system (1.1) will be computed for

$$x \in [-1, 1], \quad t = 0.05.$$

We denote the left- and right-hand states of the Riemann problem by U_L, U_R, respectively.

4.1. **Approximate the exact solution.**

In this subsection, our new scheme will be shown to maintain equilibrium states caused by stationary waves. However, the classical scheme does not. Consequently, perturbations in the classical scheme force the equilibrium state out of its equilibrium position and produces new waves.

4.1.1. *Test case 1.* Let us take the Riemann initial data

$$\begin{aligned} U_L &= (3.703475573136399, -0.209571952727429), \\ U_R &= (4.203977374422297, -0.184621499740394) \end{aligned}$$

and $a_L = 1.0, a_R = 1.5, \quad CFL = 0.7$. See Figure 2 and Figure 3.

It is easy to check that this two states U_L, U_R are the left-hand and the right-hand of a stationary contact. Our scheme is shown to give quickly the stationary contact. However, the modified Lax-Friedrich scheme approximates a visibly different function.

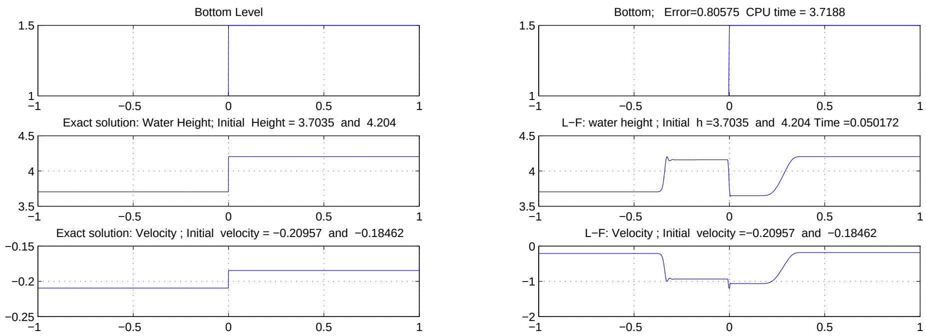

FIGURE 2. Classical scheme does not approximate the stationary wave

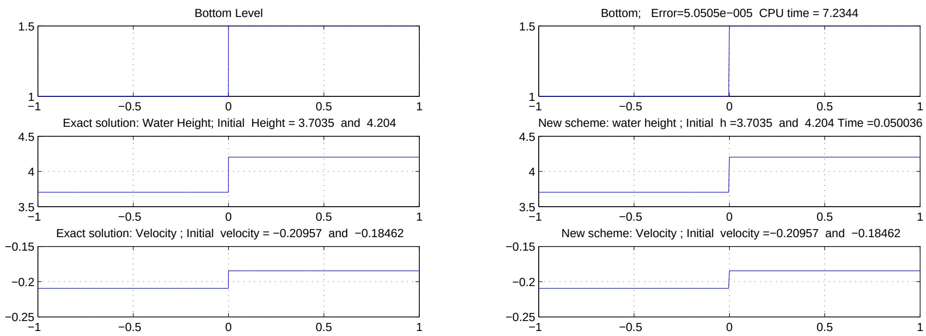

FIGURE 3. Stationary wave and its approximation by the well-balanced scheme

4.1.2. *Test case 2.* The Riemann initial data are

$$U_L = (1, 0.2),$$
$$U_R = (1.501135158120436, 0.133232506692082)$$

and $a_L = 1.0, a_R = 1.5, \quad CFL = 0.7$. See Figure 4 and Figure 5.

It is easy to check that this two states U_L, U_R are the left-hand and the right-hand of a stationary contact. Our scheme is shown to give quickly the stationary contact. However, the modified Lax-Friedrich scheme approximates a visibly different function.

4.1.3. *Test case 3.* The Riemann initial data are

$$U_L = (0.5, 2),$$
$$U_R = (1.166592483776811, 0.857197362323583)$$

and $a_L = 1.0, a_R = 1.5, \quad CFL = 0.7$. See Figure 6 and Figure 7.

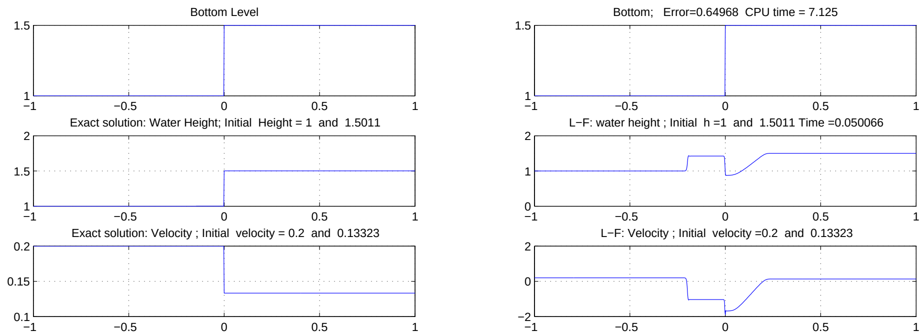

FIGURE 4. Classical scheme does not approximate the stationary wave

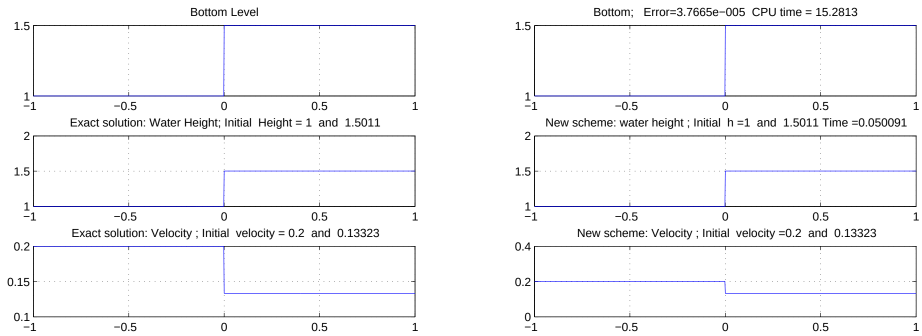

FIGURE 5. Stationary wave and its approximation by the well-balanced scheme

It is easy to check that this two states U_L, U_R are the left-hand and the right-hand of a stationary contact. Our scheme is shown to give quickly the stationary contact. However, the modified Lax-Friedrich scheme approximates a visibly different function.

4.1.4. *Test case 4.*

$$U_L = (0.5, 2), \quad U_R = (1, 0.2), \quad a_L = 1, a_R = 1.5, \quad CFL = 0.7.$$

The solution is a 1-shock followed by a stationary wave and then followed by a 2-shock. See Figure 8 and Figure 9, and Table 4.1.

N	$\|\|U_h^{\mathrm{N}} - U\|\|_{L^1}$	CPU time (s)
500	0.014021	4.6406
1000	0.0081575	16.4219
2000	0.0046675	91.375

(4.1)

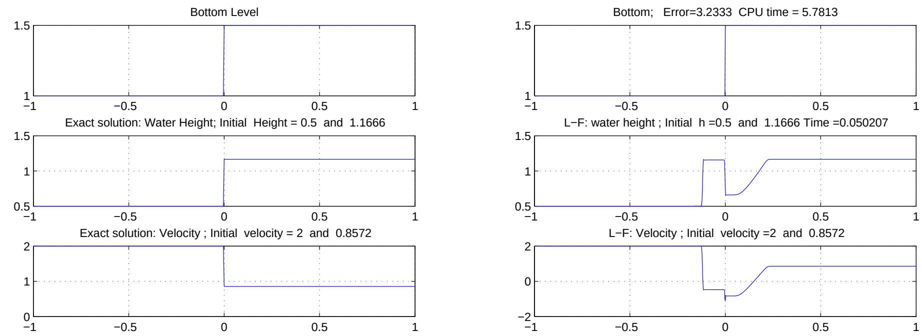

FIGURE 6. Classical scheme does not approximate the stationary wave

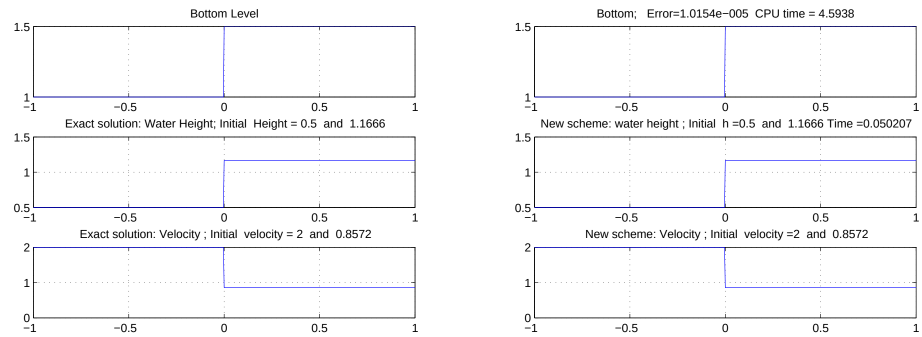

FIGURE 7. Stationary wave and its approximation by the well-balanced scheme

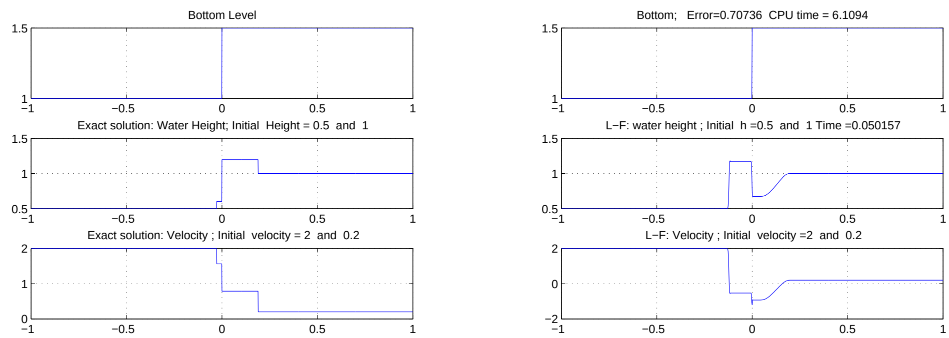

FIGURE 8. Classical scheme does not approximate the exact solution

4.2. **Better Approximations.**

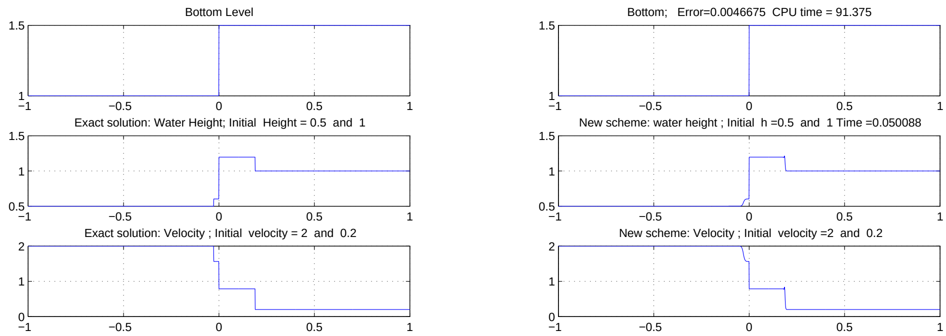

FIGURE 9. Exact solution and its approximation by the well-balanced scheme with 2000 mesh-points.

4.2.1. *Test case 1.*

$$U_L = (1, 4), \quad U_R = (2, 5), \quad a_L = 1.2, a_R = 1.3, \quad CFL = 0.7.$$

The solution is a stationary wave followed by a 1-shock wave, and then followed by a 2-rarefaction wave. See Figure 10 and Figure 11, Tables 4.2 and 4.3.

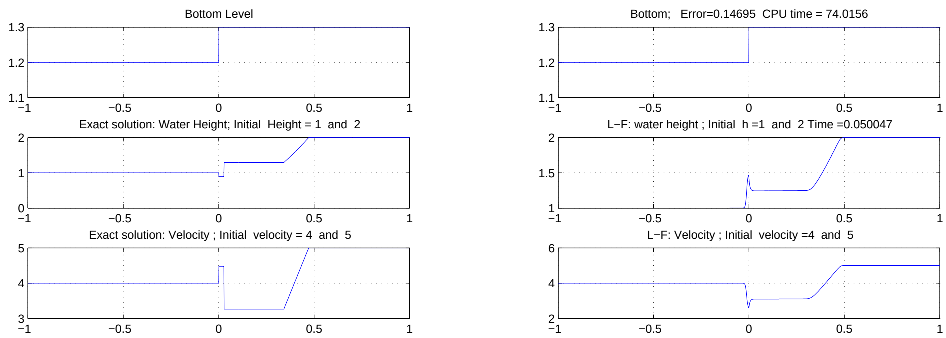

FIGURE 10. Numerical solutions by the classical scheme with 2000 mesh-points.

N	$\lvert\lvert U_h^{\mathrm{C}} - U \rvert\rvert_{L^1}$	CPU time (s)
500	0.14645	4.6406
1000	0.14454	15.2969
2000	0.14695	74.0156

(4.2)

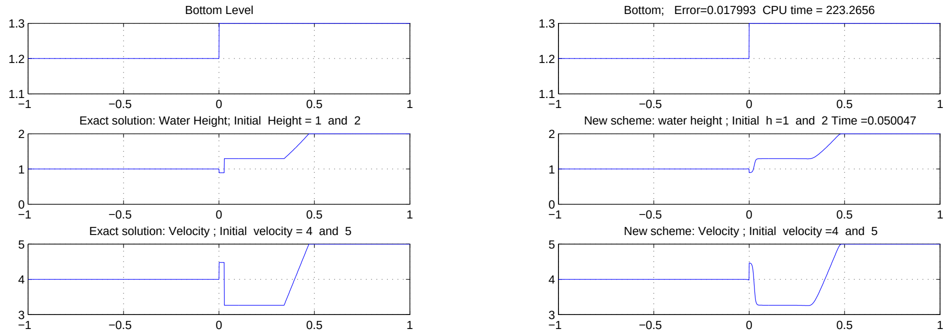

FIGURE 11. Numerical solutions by the well-balanced scheme with 2000 mesh-points.

N	$\|\|U_h^N - U\|\|_{L^1}$	CPU time (s)
500	0.057558	9.9063
1000	0.034264	38.1875
2000	0.017993	223.2656

(4.3)

4.2.2. *Test case 2.*

$$U_L = (1, -0.2), \quad U_R = (2, 0.5), \quad a_L = 1.2, a_R = 1.3, \quad CFL = 0.7.$$

The solution is a 1-shock wave followed by a stationary wave, and then followed by a 2-rarefaction wave. See Figure 12 and Figure 13, Tables 4.4 and 4.5.

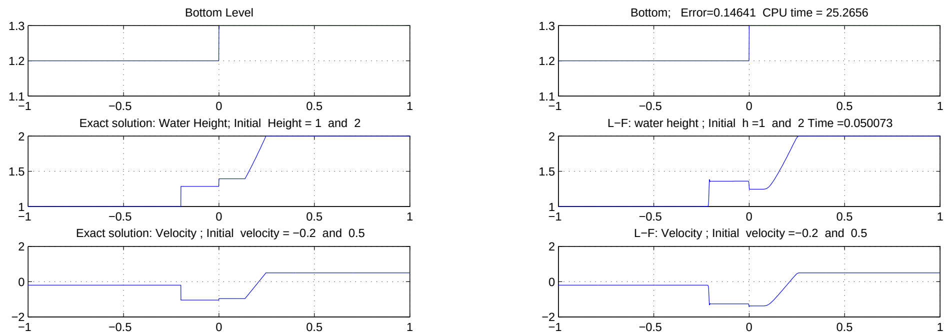

FIGURE 12. Exact solution and its approximation by the classical scheme with 2000 mesh-points.

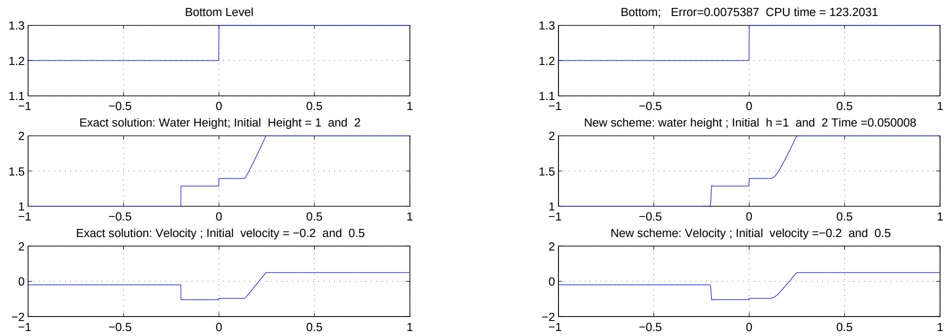

FIGURE 13. Exact solution and its approximation by the well-balanced scheme with 2000 mesh-points.

N	$\|\|U_h^{\mathrm{C}} - U\|\|_{L^1}$	CPU time (s)
500	0.44157	2.125
1000	0.15393	6.9844
2000	0.15178	36.3906

(4.4)

N	$\|\|U_h^{\mathrm{N}} - U\|\|_{L^1}$	CPU time (s)
500	0.022488	5.4688
1000	0.013109	19.3594
2000	0.0075387	123.2031

(4.5)

4.2.3. *Test case 3.*

$$U_L = (0.5, 2), \quad U_R = (1, 0.2), \quad a_L = 1, a_R = 1.5, \quad CFL = 0.7.$$

The solution is a 1-shock wave followed by a stationary wave, and then followed by a 2-shock wave. See Figure 14 and Figure 15, Tables 4.6 and 4.7.

N	$\|\|U_h^{\mathrm{C}} - U\|\|_{L^1}$	CPU time (s)
500	0.44157	2.125
1000	0.15393	6.9844
2000	0.15178	36.3906

(4.6)

N	$\|\|U_h^{\mathrm{N}} - U\|\|_{L^1}$	CPU time (s)
500	0.016451	4.5
1000	0.0086137	18.4531
2000	0.0045576	109.7969

(4.7)

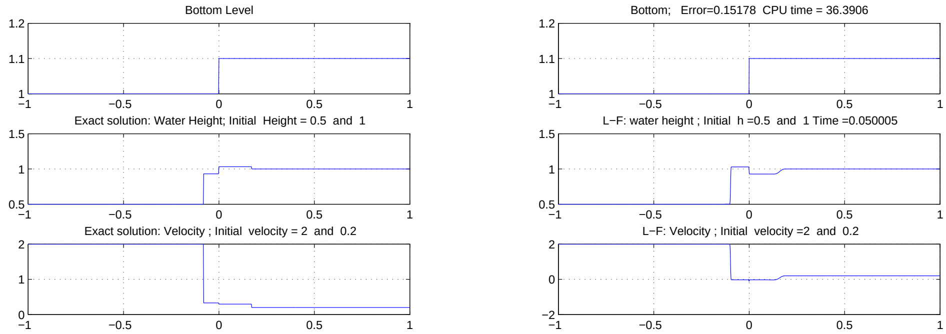

FIGURE 14. Exact solution and its approximation by the classical scheme with 2000 mesh-points.

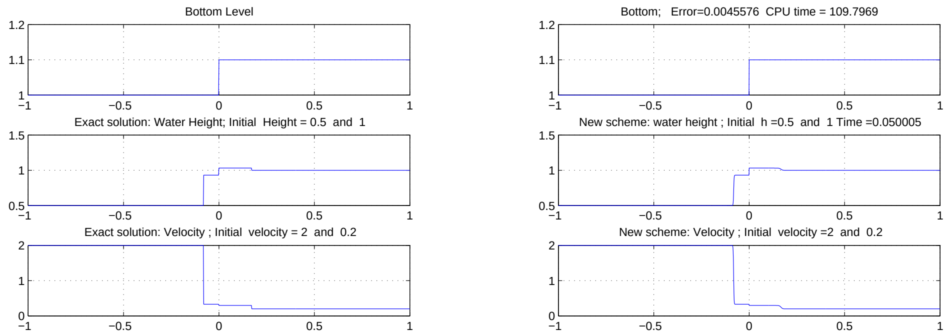

FIGURE 15. Exact solution and its approximation by the well-balanced scheme with 2000 mesh-points.

5. CONCLUSIONS

As expected, classical schemes with traditional discretizations of the right-hand side of conservation laws with source terms, and in this case the shallow water equations, give unsatisfactory results. The errors may grow when reducing the mesh size. Our scheme (3.4) is shown, by tests, to be stable and to capture stationary wave. In our scheme, errors are reduced when mesh size is reduced, and when there is a stationary wave, our scheme quickly gives that stationary wave.

Furthermore, classical schemes do not give the right solutions in many cases. Since it does not conserve the equilibrium states, it would probably force these states out of their equilibrium positions. In this situations, new waves will be formed. So classical schemes may give approximations to functions that are completely different from the exact solution (by the wave structure inside the those functions and the exact solutions). Our scheme is shown to give an appropriate approximations of the exact solutions.

References

[1] N. Andrianov and G. Warnecke, On the solution to the Riemann problem for the compressible duct flow. *SIAM J. Appl. Math.*, 64(3):878901, 2004.

[2] N. Andrianov and G. Warnecke, The Riemann problem for the BaerNunziato two-phase flow model. *J. Comput. Phys.*, 195(3):434464, 2004.

[3] E. Audusse, F. Bouchut, M-O. Bristeau, R. Klein, and B. Perthame, A fast and stable well-balanced scheme with hydrostatic reconstruction for shallow water flows. *SIAM J. Sci. Comp.*, 25(6):2050–2065, 2004.

[4] F. Bouchut, *Nonlinear stability of finite volume methods for hyperbolic conservation laws and well-balanced schemes for sources.* Frontiers in Mathematics. Birkhäuser Verlag, Basel, 2004.

[5] R. Botchorishvili, B. Perthame, and A. Vasseur, Equilibrium schemes for scalar conservation laws with stiff sources. *Math. Comput.*, 72:131–157, 2003.

[6] R. Botchorishvili and O. Pironneau, Finite volume schemes with equilibrium type discretization of source terms for scalar conservation laws. *J. Comput. Phys.*, 187:391–427, 2003.

[7] G. Dal Maso, P.G. LeFloch, and F. Murat, Definition and weak stability of nonconservative products. *J. Math. Pures Appl.*, 74:483–548, 1995.

[8] P. Goatin and P.G. LeFloch, The Riemann problem for a class of resonant nonlinear systems of balance laws. *Ann. Inst. H. Poincar Anal. NonLinéaire*, 21:881–902, 2004.

[9] L. Gosse, A well-balanced flux-vector splitting scheme designed for hyperbolic systems of conservation laws with source terms. *Comp. Math. Appl.*, 39:135–159, 2000.

[10] J.M. Greenberg and A.Y. Leroux, A well-balanced scheme for the numerical processing of source terms in hyperbolic equations. *SIAM J. Numer. Anal.*, 33:1–16, 1996.

[11] J.M. Greenberg, A.Y. Leroux, R. Baraille, and A. Noussair, Analysis and approximation of conservation laws with source terms. *SIAM J. Numer. Anal.*, 34:1980–2007, 1997.

[12] E. Isaacson and B. Temple, Nonlinear resonance in systems of conservation laws. *SIAM J. Appl. Math.*, 52:1260–1278, 1992.

[13] E. Isaacson and B. Temple, Convergence of the 2×2 godunov method for a general resonant nonlinear balance law. *SIAM J. Appl. Math.*, 55:625–640, 1995.

[14] S. Jin and X. Wen, *An efficient method for computing hyperbolic systems with geometrical source terms having concentrations,* J. Comput. Math., 22 (2004), pp. 230–249.

[15] D. Kröner and M.D. Thanh, Numerical solutions to compressible flows in a nozzle with variable cross-section. *SIAM J. Numer. Anal.*, 43(2):796–824, 2005.

[16] D. Kröner and M.D. Thanh, On the Model of Compressible Flows in a Nozzle: Mathematical Analysis and Numerical Methods. *Proc. Tenth. Intern. Conf. Hyp. Prob. (HYP04), Osaka, Yokohama Publishers*, pages 117–124, 2006.

[17] P.D. Lax, Shock waves and entropy, in: E.H. Zarantonello, Ed.,. *Contributions to Nonlinear Functional Analysis*, pages 603–634, 1971.

[18] P.G. LeFloch, Shock waves for nonlinear hyperbolic systems in nonconservative form. *Institute for Math. and its Appl., Minneapolis, Preprint*, 593, 1989.

[19] P.G. LeFloch and M.D. Thanh, The Riemann problem for fluid flows in a nozzle with discontinuous cross-section. *Comm. Math. Sci.*, 1(4):763–797, 2003.

[20] P.G. LeFloch and M.D. Thanh, The Riemann problem for shallow water equations with discontinuous topography. *Comm. Math. Sci.*, (accepted).

[21] D. Marchesin and P.J. Paes-Leme, A Riemann problem in gas dynamics with bifurcation. Hyperbolic partial differential equations III. *Comput. Math. Appl. (Part A)*, 12:433–455, 1986.

Mai Duc Thanh
Department of Mathematics, International University, Quarter 6, Linh Trung Ward, Thu Duc District, Ho Chi Minh City, Vietnam
E-mail address: mdthanh@hcmiu.edu.vn

Md. Fazlul Karim
School of Mathematical Sciences, Universiti Sains Malaysia, 11800 USM, Pulau Pinang, Malaysia.
E-mail address: mdfazlulk@yahoo.com

Ahmad Izani Md. Ismail
School of Mathematical Sciences, Universiti Sains Malaysia, 11800 USM, Pulau Pinang, Malaysia.
E-mail address: izani@cs.usm.my